

Effects of microstructure on the sky-green color in imitating ancient Jun glazes

Jianfeng ZHU,[†] Pei SHI,^{††} Fen WANG, Longlong DONG and Ting ZHAO

School of Materials Science and Engineering, Shaanxi University of Science & Technology, Xi'an 710021, China

The sky-green glaze of ancient Jun ware was successfully imitated with the addition of 4 wt % calcium phosphate for introducing the phosphorus (P) to the composition. Effects of the calcium phosphate contents on the chromaticity, precipitated phase and microstructure of sky-green glaze were investigated. Based on the analysis of colorimeter, XRD, FT-IR, XPS and SEM, a possible coloring mechanism was proposed to explain the variation of glaze colors with the increasing of calcium phosphate content. The results indicated that the addition of calcium phosphate contributed to increasing the content of calcium iron phosphate $[Ca_{19}Fe_2(PO_4)_{14}]$ and the size of phase separation droplets in glazes. The formation of $Ca_{19}Fe_2(PO_4)_{14}$ decreased the ratio of Fe^{2+} to Fe^{3+} and the increased size of phase separation droplets weakened the structural color, which increased the L^* and b^* value of glazes. Therefore, the color of sky-green glaze got more green and white gradually.

©2016 The Ceramic Society of Japan. All rights reserved.

Key-words : Sky-green glaze, Calcium phosphate, Microstructure, Structural color, Imitating Jun glaze

[Received May 15, 2015; Accepted October 15, 2015]

1. Introduction

Jun ware, produced in Yuzhou, Henan Province, is one of the five famous wares (Jun, Ru, Guan, Ge and Ding ware) in the Chinese Song Dynasty (AD 960-1279).¹⁾ Jun Guan ware has long enjoyed a very high reputation with phantasmagoric glaze colors. In which, purplish-red and purplish-blue series are two representative colors. Especially, the purplish-blue series exhibit blue of different intensities and have more complex coloring mechanism.²⁾ According to the depth of blue, it can be classified into sky-blue, sky-green and moon-white glaze, etc. However, what makes the difference in them still need to be studied at some length.

Previous studies have shown that Fe_2O_3 content has a huge influence on the glaze color and the optimum content is about 2.5 wt % in sky-green Jun glaze. Additionally, the microstructure is also an important factor affecting the glaze color.²⁾ And a lot of efforts have been focused on the microstructure of glaze to find the further coloring mechanism. W. D. Kingery³⁾ found that the inhomogeneous structure could lead to scattering and reflection of light, so blue opalescence was formed on Jun glaze surface. Chen et al.⁴⁾ confirmed that the inhomogeneous structure was actually liquid-liquid phase-separation structure, and the blue opalescence of Jun glaze originated from scattering of droplets in separative-phase glaze. And they also investigated that the blue opalescence was brighter when the average size of discrete droplets was 100 nm.⁵⁾ Some scholars suggested that unmelted raw materials, such as residual cristobalite and calcium phosphate particles, and many tiny bubbles (1–2 mm) would also play a role in the formation of the blue opalescence in Jun glaze.^{6,7)} All of the analyses show that phase-separation structure is the origin of blue opalescence of Jun glaze, and the size of phase separation droplets determines the color intensity of blue opalescence.

However, which items in the composition affect the microstructure and glaze color more intensively still need to be confirmed.

In addition, researches show that the P content has a major influence on the glaze color of Jun ware.⁶⁾ The P is basically introduced by calcined bone ash in ancient ware, which has the disadvantages of hard control of glaze compositions and environmental pollution.⁸⁾ With calcium phosphate replacing calcined bone ash, it is not only easy to control of glaze compositions but also good for environmental protection.

In this work, calcium phosphate was utilized as the promoter of phase separation to imitate the sky-green glaze of ancient Jun ware in the R_2O - RO - Al_2O_3 - SiO_2 - P_2O_5 base system. The effects of calcium phosphate contents on the evolution of crystalline phase and phase separation of the sky-green glaze were investigated in detail. The coloring changing mechanism about the sky-green glaze color was also discussed.

2. Experimental procedures

2.1 Glaze preparation

Chemical compositions of the raw materials are given in **Table 1**. Based on the ancient sky-green Jun glaze (Liujiamen Jun Kiln) compositions (**Table 2**) which were measured by ourselves, the base glaze compositions were made by 60 wt % of Na-feldspar, 21 wt % of quartz sand, 15 wt % of calcite, 2 wt % of talc, 2 wt % of kaolin and 0–12 wt % of calcium phosphate. Meanwhile 2 wt % of commercial grade iron oxide was added as the colorant.

The raw glaze slurry was prepared by directly milling the starting materials which was weighted before with 70 wt % water, 0.8 wt % sodium carboxyl methyl cellulose (CMC), 0.3 wt % sodium tripolyphosphate (STP) and milled at a rate of 300 r/min for 35 min. The glaze slip was sieved and the density was adjusted to 1.5 g/cm³ by water. Then the glaze slip was applied to the biscuits test piece (\varnothing 4–5 cm) by dipping. After dried, the test pieces were fired at a heating rate of 3°C/min to 900°C and 1°C/min to 1300°C, and then insulated for 20 min at this tem-

[†] Corresponding author: J. Zhu; E-mail: zhujf@sust.edu.cn

^{††} Corresponding author: P. Shi; E-mail: shipei7121@163.com

^{†††} Preface for this article: DOI <http://dx.doi.org/10.2109/jcersj2.124.P1-1>

Table 1. Chemical compositions of the raw materials (wt %)

Raw materials	SiO ₂	Al ₂ O ₃	Fe ₂ O ₃	CaO	MgO	K ₂ O	Na ₂ O	Ca ₃ (PO ₄) ₂
feldspar	69.94	17.41	0.51	3.54	1.01	0.51	7.08	—
quartz	98.37	1.41	0.22	—	—	—	—	—
calcite	0.67	—	—	98.68	0.65	—	—	—
talc	64.64	—	0.06	0.24	34.96	0.06	0.04	—
kaolin	52.94	45.46	0.57	0.36	0.11	—	—	—
calcium phosphate	—	—	—	—	—	—	—	99.9

Table 2. Chemical compositions of ancient Jun glaze

SiO ₂	Al ₂ O ₃	Fe ₂ O ₃	CaO	MgO	K ₂ O	Na ₂ O	P ₂ O ₅	
wt %	65.90	9.71	2.68	14.33	2.37	2.79	1.67	0.55

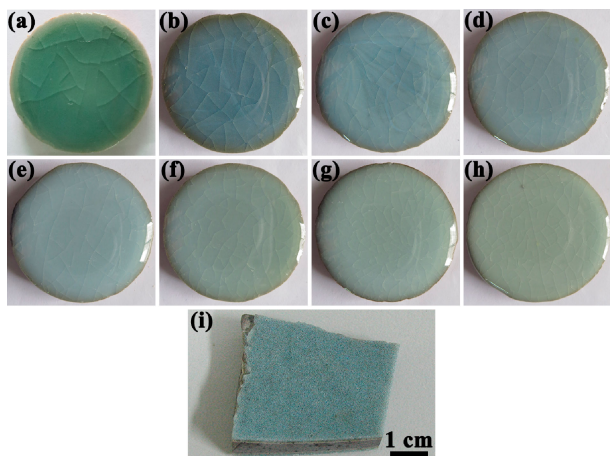


Fig. 1. Appearance of imitating and ancient Jun glazes, (a)–(h) different calcium phosphate contents of 0, 2, 4, 6, 8, 10, 12 and 14 wt%; (i) Ancient sky-green Jun glaze.

perature under a reducing atmosphere. Finally, the samples were cooled down to room temperature naturally.

2.2 Characterization

The color parameters (L^* , a^* , b^*) for the fired specimens were measured using the WSD-3C colorimeter. And the phase composition of the test pieces was identified by X-ray diffraction (XRD) using a D/max 2200PC X-ray diffractometer (Japan) with Cu K α radiation ($\lambda = 1.5406 \text{ \AA}$). Meanwhile the samples were measured at a scanning rate of $8^\circ/\text{min}$ in the 2θ range of 10 – 60° under 40 kV and 100 mA . The infrared spectra at 400 – 1200 cm^{-1} were characterized by a Spectrum One FT-IR spectrometer (VERTE70) using the KBr standard pellet method. The chemical analysis was performed on an ESCALAB MKII X-ray photoelectron spectrometer (VG Scientific, UK) using Al K α radiation. The microstructure of the samples was investigated by scanning electron microscopy (SEM, Hitachi, S-4800) equipped with energy dispersive spectrometry (EDS). Before the testing, the surface of the samples was etched using 10 vol % HF for 30 s to expose the crystal and phase separation structures.

3. Results and discussion

Figures 1(a)–1(h) shows the typical glaze colors depending on the contents of calcium phosphate. And the color values (a^* , b^*) and lightness (L^*) parameters (whiteness) are listed in Table 3. As being observed, the L^* values increased with the increase of

Table 3. L^* , a^* and b^* values and glaze colors according to different calcium phosphate contents

Ca ₃ (PO ₄) ₂ (wt %)	a [*]	b [*]	L [*]	Color
0	-7.97	2.92	37.87	Olive-green
2	-7.24	7.93	49.09	Sky-blue
4	-9.00	-5.58	55.46	Sky-green
6	-7.00	-3.40	56.45	Moon-white
8	-7.34	-3.24	63.44	Moon-white
10	-6.61	-0.55	58.05	Pea-green
12	-7.09	1.03	63.90	Pea-green
14	-6.85	0.96	64.59	Pea-green

calcium phosphate content. In addition, negative values of a^* and positive values of b^* were measured from the glazes with 0–2 and 12–14 wt % calcium phosphate addition, indicating that the values lay in the upper left quadrant (green and yellow region) with coordinates, and at the same time, negative values of a^* and negative values of b^* were measured from the glazes with 4–10 wt % calcium phosphate addition, indicating that the values lay in the under left quadrant (green and blue region) with coordinates. Hence, it was found that the amount of calcium phosphate was a main factor of the L^* and b^* values in the present system. Besides, the colors of samples were similar to the sky-blue, sky-green (i) and moon-white glaze colors of ancient Jun ware when the calcium phosphate contents were 2, 4 and 6–8 wt %, respectively.

Figure 2 shows the XRD patterns of the glazes with different calcium phosphate contents. There were only amorphous phase in the glazes that contained 0–2 wt % calcium phosphate [Figs. 2(a) and 2(b)]. Whereas Ca₁₉Fe₂(PO₄)₁₄ crystal phases emerged at 31.17 and 34.55° peaks in the glazes containing 4–8 wt % calcium phosphate [Figs. 2(c)–2(e)], and the glazes with 10–14 wt % calcium phosphate [Figs. 2(f)–2(h)] displayed two major crystalline phases, whitlockite [Ca₃(PO₄)₂] with main peaks at 31.13 and 34.47° and a small amount of Ca₁₉Fe₂(PO₄)₁₄. Furthermore, as the calcium phosphate contents increased, the peak intensity of crystalline phase and the opacity of glazes were also increased.

Figure 3 displays the SEM images of glazes with 4, 8, 10, 14 wt % calcium phosphate, respectively. In which, the irregular shaped crystals were observed in every sample. The EDS analysis results are presented in Table 4, measured on the microspots denoted by the numbers 1–4 in the SEM images of crystals (Fig. 3). It showed that the crystals in position 1 and 2 were rich in Fe, Ca, P and O, whereas the crystals in position 3 and 4 were rich in Ca, P and O. The XRD pattern in Fig. 2 proved that the irregular shaped crystals were Ca₁₉Fe₂(PO₄)₁₄ when the calcium phosphate contents were 4 and 8 wt %, and Ca₃(PO₄)₂ was also precipitated when the calcium phosphate contents were 10 and 14 wt %.

According to some researches from Zhang et al.^{9,10} the structure of Fe³⁺–O–Fe²⁺ was the essence of iron-colored glass,

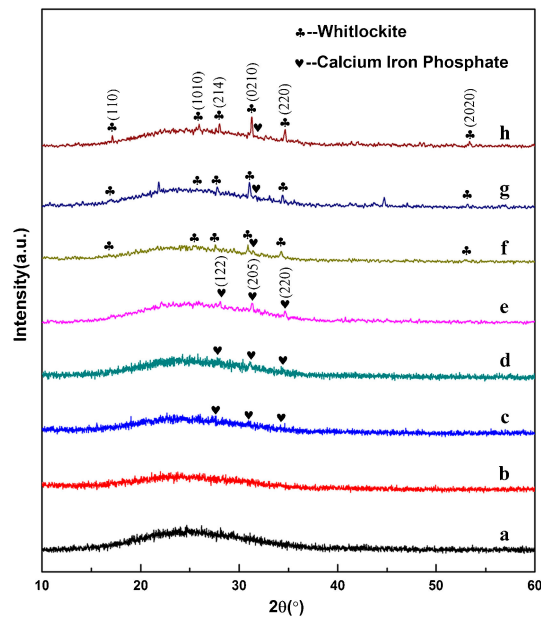


Fig. 2. XRD patterns of glazes, a-h different calcium phosphate contents of 0, 2, 4, 6, 8, 10, 12 and 14 wt%.

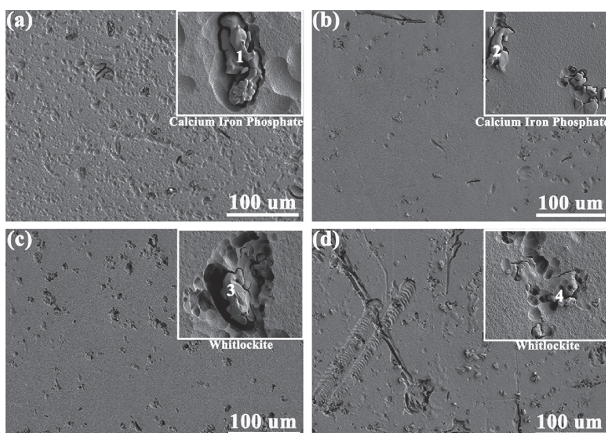


Fig. 3. SEM images of crystals on the glaze surfaces, (a)-(d) correspond to calcium phosphate contents of 4, 8, 10, and 14 wt% in glazes.

Table 4. Element compositions of precipitated crystals measured at the points indicated in Fig. 3

Crystal	C	O	Na	K	Mg	Al	Si	P	Ca	Fe
1	4.42	19.02	1.44	1.40	1.64	2.28	6.40	17.79	26.33	19.28
2	4.42	20.28	1.07	1.07	1.51	1.84	5.76	19.75	32.10	12.20
3	4.41	24.55	1.09	2.07	1.27	1.55	7.05	21.29	35.43	1.29
4	4.40	20.68	1.03	2.17	1.35	1.87	7.75	21.71	37.81	1.25

and more Fe^{2+} could make color of glass get bluer under a reducing atmosphere. Hence, with the increasing of the content of generated $\text{Ca}_{19}\text{Fe}_2(\text{PO}_4)_{14}$, the Fe^{2+} content in the glazes decreased, which led to the glaze colors become lighter. However, as shown in Figs. 1(a)-1(h), the glaze colors with the addition of calcium phosphate got bluer than the glaze without calcium phosphate. Consequently, the glaze colors with calcium phosphate had not only the coloration of iron.

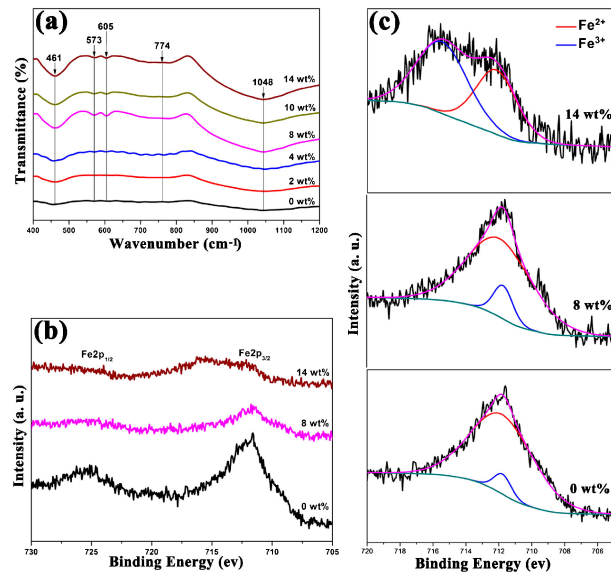
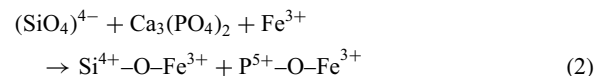
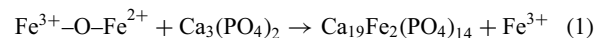


Fig. 4. (a) FT-IR spectrum, (b) Fe2p XPS spectra and, (c) Fitting spectra of the Fe2p 3/2 peaks of the glazes with different calcium phosphate contents.

By comparing the glaze colors and phases with different calcium phosphate contents at the same firing temperature, the glazes in which the calcium phosphate contents were respectively 0, 2, 4, 8, 10 and 14 wt% would be researched further.

FT-IR spectrum of the studied glazes is showed in Fig. 4(a). The results showed that the main features were five bands at 1048, 774, 605, 573 and 461 cm⁻¹, respectively. The bands at 1048 and 461 cm⁻¹ were assigned to the stretching vibration of Si-O bonds.¹¹⁾ The absorption band at 774 cm⁻¹ could correspond to the $(\text{PO}_4)^{3-}$ asymmetric stretches of P-O-P bond.^{12,13)} And the low-frequency absorption bands at 605 and 573 cm⁻¹ might be assigned to Fe-O stretching vibration.^{14,15)} Additionally, with increasing the $\text{Ca}_3(\text{PO}_4)_2$ crystal content, the stretching vibration of Si-O and Fe-O bonds and the asymmetric stretches of P-O-P all increased. It was suggested that broken silica tetrahedrons and $\text{Fe}^{3+}-\text{O}-\text{Fe}^{2+}$ structures became more when calcium phosphate content was increased. Spectroscopic studies had shown that iron ions in the calcium iron phosphate glasses could form stable P-O-Fe covalent bonds, so $\text{P}^{5+}-\text{O}-\text{Fe}^{3+}$ bond was formed in the glazes.^{13,16)} Moreover, the phosphorus-oxygen tetrahedron replaced P-O-P linkages, which weakened the cross-linking of the glass network.¹³⁾ As a result, the viscosity of molten glazes decreased with the increase of calcium phosphate content. The main reactions are expressed by Eqs. (1) and (2) as following:



The surface element analysis of the glazes with 0, 8 and 14 wt% calcium phosphate is illustrated in Fig. 4(b). And from Fig. 4(b), the XPS binding energy peaks of Fe 2p1/2 and Fe 2p3/2 appeared at 712.1 and 725.49 eV.¹⁷⁾ The broad Fe 2p3/2 peaks suggested the coexistence of Fe^{2+} and Fe^{3+} in samples.¹²⁾ The fitting spectra of the Fe 2p3/2 peaks are displayed in Fig. 4(c), where the binding peaks were fitted by Lorentzian-Gaussian functions. It was found that the Fe^{2+} concentration decreased obviously with the increasing of the calcium phosphate

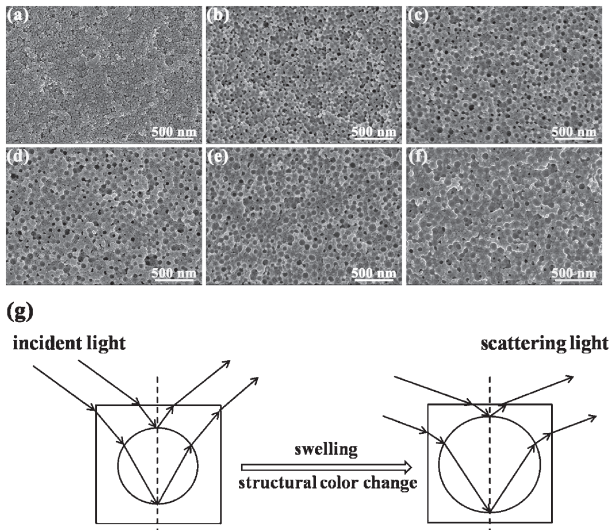


Fig. 5. Typical SEM images of separation structures on the sample surfaces, (a)–(f) different calcium phosphate contents of 0, 2, 4, 8, 10 and 14 wt %; (g) the concept of the change of the structural color by swelling the separation structure.

Table 5. Effect of different calcium phosphate contents on the average size of phase separation droplets

$\text{Ca}_3(\text{PO}_4)_2/\text{wt}\%$	0	2	4	8	10	14
droplet size/nm	0	46	66	71	72	85

content. The Fe^{2+} to Fe^{3+} atomic ratios of glazes were 93.53/6.47, 88.38/11.62 and 42.26/57.74, respectively. Therefore, the XPS results further confirmed that the calcium phosphate was helpful to reduce the Fe^{2+} concentration in glazes, which could make glaze colors turn yellow gradually.

Figure 5 presents the SEM micrographs of samples with different calcium phosphate contents of 0, 2, 4, 8, 10 and 14 wt %. As shown in Fig. 5(a), the glaze did not have the liquid-liquid phase separation structure, and even the discrete droplet phase separation structures were formed in Figs. 5(b)–5(f).¹⁸⁾ 60 discrete droplet phase separation structures were chosen randomly from Figs. 5(a)–5(f) to investigate the average size of phase separation droplets by the Image-Nano Measurer software. As depicted in Table 5, the size of phase separation droplets was the smallest when the content of calcium phosphate was 2 wt %. With 4–10 wt % calcium phosphate, the size of droplets did not change and the density decreased. Furthermore, the size of droplets was the largest with 14 wt % calcium phosphate. The reason for this was that, the viscosity of molten glazes decreased when the content of calcium phosphate increased. Therefore, the movement speed of particles got faster so that discrete phase was easy to move to the surface of phosphate glass.¹⁹⁾

Due to a three-dimensional amorphous structure of the short-range order instead of the long-range order in the separative-phase glaze, it was the main source of the structural color. The structural color of object was caused by optical effects developed by microstructure such as interference, diffraction and reflection when the size range of the object was comparable to the optical wavelength range.^{20,21)} The developing color strongly depended on the refractive index and the size of periodic structure.²¹⁾ Its color rendering principle could be analyzed by the Rayleigh scattering. When the size of scattering ions was 1–300 nm, the

Rayleigh scattering might occur on glaze surface. The scattering intensity was determined with the following formulas:^{22,23)}

$$I(\lambda)_{\text{scattering}} \propto \frac{I(\lambda)_{\text{incident}}}{\lambda^4} \quad (3)$$

Where $I(\lambda)_{\text{incident}}$ is the incident intensity and λ is the incident light wavelength. As λ is smaller, the Rayleigh scattering developed more easily. Since blue light was at the short wavelength end of the visible spectrum, it was scattered in the atmosphere much more than the longer-wavelength red light. As a result, the structural color developed by the Rayleigh scattering showed blue and the glazes color became blue with addition of calcium phosphate.²⁴⁾ When the size of phase separation droplets became larger, the scattering intensity [$I(\lambda)_{\text{incident}}$] was smaller and the opalescence blue which was formed by structural color was lighter, as shown in Fig. 5(g). So the blue of glaze surfaces were lighter with the increasing of the calcium phosphate content. According to the research from Chen et al.,²⁵⁾ the Fe_2O_3 was gathered in the phase separation droplets so that the refractive indices between base phase and phase separation droplets got larger. As a result, the structural color darkened with addition of Fe_2O_3 . Based on the trichromatic theory, the composite color of the yellow and the blue was green.²⁶⁾ Therefore, the glaze surfaces were pea-green when the calcium phosphate contents were 10–14 wt %.

4. Conclusions

The sky-green glaze of ancient Jun ware was successfully imitated with the addition of 4 wt % calcium phosphate. With increasing of the calcium phosphate content, $\text{Ca}_{19}\text{Fe}_2(\text{PO}_4)_{14}$ was formed so that the opacity of glazes improved while the ratio of Fe^{2+} to Fe^{3+} in glazes decreased. The SEM microstructure showed that the discrete droplet phase separation structures were developed in glazes and their sizes were less than 100 nm, so the structural color was formed owing to the Rayleigh scattering. A dual coloring changing mechanism with the increasing of the calcium phosphate content was in effect for the sky-green glaze of imitating ancient Jun porcelain, covering the precipitated crystals and the varying size of phase separation droplets. Besides, the chemical color of Fe_2O_3 was main coloring factor, and the structural color formed by phase separation droplet played a role in auxiliary coloring in the glaze.

Acknowledgements This work was supported by the National Natural Science Foundation of China (51472153), the Key Project of State Administration of Culture Heritage, China (20120218), Research and Application of Ceramic Glaze Prepared with Mineral Waste Residue, China (2012KTDZ02-01-03), and the Graduate Innovation Fund of Shaanxi University of Science and Technology.

References

- 1) J. Z. Li, "History of Ancient Science and Technology (Ceramics part)", Science Press, Beijing, (1998).
- 2) F. Wang, J. M. Miao, J. Y. Hou, Y. Lin and J. F. Zhu, *Palace Museum Journal*, 3, 100–108 (2012).
- 3) W. D. Kingery and P. B. Vandiver, *Studio Potter*, 14, 23–26 (1986).
- 4) X. Q. Chen, R. F. Huang and S. P. Chen, *J. Chin. Ceram. Soc.*, 9, 245–252 (1981).
- 5) X. Q. Chen, R. F. Huang, S. P. Chen, X. Y. Song and X. L. Zhou, *J. Chin. Ceram. Soc.*, 2, 129–140 (1983).
- 6) W. D. Kingery and P. B. Vandiver, "Ceramic Masterpieces: Art, Structure and Technology", Free Press, New York (1983).

- 7) J.-Y. Kim, H. No, A. Y. Jeon, U. Kim, J.-H. Pee, W.-S. Cho, K. J. Kim, C. M. Kim and C. S. Kim, *Ceram. Int.*, 37, 3389–3395 (2011).
- 8) W. D. Li, J. Z. Li, Z. Q. Deng, J. Wu and J. K. Guo, *Ceram. Int.*, 31, 487–494 (2005).
- 9) C. W. Zhang, *Glass & Enamel*, 32, 38–42 (2004).
- 10) B. Li, C. Q. Wang, W. Liu, M. Ye and N. Wang, *Mater. Lett.*, 90, 45–48 (2013).
- 11) I. Kansal, A. Goel, D. U. Tulyaganov, R. R. Rajagopal and J. M. F. Ferreira, *J. Eur. Ceram. Soc.*, 32, 2739–2746 (2012).
- 12) R. K. Brow, *J. Non-Cryst. Solids*, 263–264, 1–28 (2000).
- 13) H. J. Li, X. F. Liang, C. L. Wang, H. J. Yu, Z. Li and S. Y. Yang, *J. Mol. Struct.*, 1067, 154–159 (2014).
- 14) O. Cozar, N. Leopold, C. Jelic, V. Chiş, L. David, A. Mocanu and M. Tomoaia-Cotîşel, *J. Mol. Struct.*, 788, 1–6 (2006).
- 15) M. Gotić and S. Musić, *J. Mol. Struct.*, 834–836, 445–453 (2007).
- 16) L. Ma, R. K. Brow and A. Choudhury, *J. Non-Cryst. Solids*, 402, 64–73 (2014).
- 17) T. Yamashita and P. Hayes, *Appl. Surf. Sci.*, 254, 2441–2449 (2008).
- 18) E. Bou, A. Moreno, A. Escardino and A. Gozalbo, *J. Eur. Ceram. Soc.*, 22, 1791–1796 (2007).
- 19) F. J. Torres and J. Alarcón, *J. Eur. Ceram. Soc.*, 25, 349–355 (2005).
- 20) S. Kinoshita and S. Yoshioka, *ChemPhysChem*, 6, 1442–1459 (2005).
- 21) K. Higashiguchi, M. Inoue, T. Oda and K. Matsuda, *Langmuir*, 28, 5432–5437 (2012).
- 22) R. Thalman, K. J. Zarzana, M. A. Tolbert and R. Volkamer, *J. Quant. Spectrosc. Ra.*, 147, 171–177 (2014).
- 23) F. Wang, H. J. Luo, Q. Li and W. D. Li, *J. Chin. Ceram. Soc.*, 37, 181–186 (2009).
- 24) Y. M. Yang, M. Feng, X. Ling, Z. W. Mao, C. S. Wang, X. M. Sun and M. S. Guo, *J. Archaeol. Sci.*, 32, 301–310 (2005).
- 25) X. Q. Chen, R. F. Huang, J. Sun, S. P. Chen and M. L. Ruan, *J. Chin. Ceram. Soc.*, 12, 236–242 (1984).
- 26) A. Choudhury, “Principles of Colour and Appearance Measurement”, Woodhead Publishing (2014).